ENGINEERING PERSPECTIVE

CONTENTS

ENGINEERING PERSPECTIVE Volume: 1 Issue: 3 30 September 2021

e-ISSN: 2757-9077

Open Access

ENGINEERING PERSPECTIVE

An International Journal

Volume: 1 Issue: 3 30 September 2021

https://sciperspective.com

Engineering Perspective 1 (3): 86-91, 2021

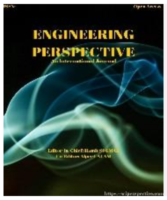

e-ISSN:2757-9077

ENGINEERING PERSPECTIVE

https://sciperspective.com/

Research Paper

Development and fabrication of vehicle body paints mixing machine

Frederic Musabyimana[1], Pacifique Turabimana[2*]

[1]*Department of Mechanical Engineering, Automobile Technology, IPRC Kigali/Rwanda Polytechnic, Kigali Rwanda*
[2]*Department of Mechanical Engineering, Automobile Technology, IPRC Gishari/Rwanda Polytechnic, Rwamagana Rwanda*

ABSTRACT

The exterior surface attractive appearance of every designed and the fabricated machine includes the vehicles is determined by the type of paint color it has to the one who takes its looks. The well-painted machine is added its value to the customers from its physical outer appearance. High attractive paint color from paint mixing activities plays an important role in the production mechanism of any attractive exterior surfaces have done by the painter industries and auto body repair companies. In some developing countries with a low percentage of industries including Rwanda, finding a standardized auto-body paint mixing machine is very expensive. Then, auto-body repair and painters in different vehicle repair industries and garages try to mix paints by using their hands without other assistance which is known as manual auto-paint mixing operation. However, this manual mixing method has several disadvantages like unattractive paint colors, low painting quality outputs, unresisting paint to solar, and rain which reduce the product's value. During the mixing operation, their hands' skin being unhealthy because of the chemicals from the paints and respiration system affected by paint smell. This method takes more time during mixing but resulted in a non-uniformity of mixed paint. Therefore, this research aim is to design and implement a paint mixing machine with accurate paint color at an affordable cost. The machine is fabricated using the materials which are available on local markets. This machine will offer more benefits to the vehicle repair companies, vehicle sellers, and dealers such as time reduction taken during vehicle body painting, more customers, the confidentiality of taking the used vehicles to the markets.

Keywords: electric engine, modelling of an electric vehicle, simulation, Matlab/Simulink, NEDC, electric vehicle, electrical bus

History
Received: 12.06.2021
Accepted: 30.08.2021

Author Contacts
*Corresponding Author
e-mail addresses : pacifique.turabimana@aait.edu.et, fredmusa2018@gmail.com
Orcid numbers : 0000-0003-2422-9056, 0000-0001-9164-6648

http://dx.doi.org/10.29228/eng.pers.52083

1. Introduction

The Paint mixers demand a design that balances time and uniformity of different paint colors during painting operation to the good body color appearance. The automobile researchers are always thinking about the vehicle body surface as one of the parameters to identify a vehicle to another. It is also protecting the vehicles against fading from the sun rays UV and facilitate vehicle body repair and maintenance in a simple way [1]. The vehicle body repaired from different garages are distinguished according to their paint colors' quality which are generated to the technicity of body painting service and the paints coat control has used during painting operation [2].

The vehicle repair industries and researchers are continually trying different technologies deal with vehicle body paint uniformity and Yong-Hee Han with his colleagues in 2003 come up with the research of developing a paint coating technology where a unique polymer layer with iron oxide particles is applied to the vehicle body during vehicle body painting. The vehicle color is defined by the vehicle type and its uses and interpreted by the human eyes. And their research identifies that painting a vehicle with different paints color to the original one during maintenance is more costly. Vehicle body paint mechanism and paint mixing colors are more expensive [3]. The vehicle coatings and the methods used to coat vehicle surfaces are identified by applied technologies. The purpose is to get the vehicle's body appearance exceeding the customers' expectations. The mixing operation should meet the high paint mixing efficiency and fulfill the environmental regulations. From these parameters, different vehicle body paint mixing methods have been developed by different researchers as the main key to make a good surface appearance [4].

The first method of paint mixing operation was the pure manual. The paints with different colors were mixed in one container to have one species' paint used to the vehicle body like the building painting operation. It takes time to have an attractive paint color for the customers. And getting the color quality standard is also not possible with this method. Hence this manual method, plastic or a wooden stick material is used to mix paints in a container by hands during agitation [5] and [6]. The output paint color is not attractive to this mixing method. The mixing of different paint colors to a large quantity manually demands more energy to operate. There is no way of measuring the output efficiency, environmental impact, and coating factor resistance to high temperature during more sun lens and low temperature and snow. The process of mixing is an important operation for auto body coating. This method plays a big role in having a well-defined body coat. The paints to be mixed are bought in liquid or powder and play the same roles to the body surface. However, for automotive paints, the liquid is mostly used.

The automotive industries and the researchers developed the mixing machines as an alternative good solution to the manual mixing method. During this period, the liquid auto-body paint mixing steps have been elaborated and classified into five phases. The phases are reactions, blending homogenization, emulsion preparation, dissolution, and paint extraction. The electrically operated paints mixing machine has developed with highly accurate and good appearance of vehicle paint color [7]. The mixing of paint powders is operated differently from the liquid mixing process. It needs to be done by rigorous shaking and creating turbulence that makes paints uniform of the paint's particles. Hence, the powder paints are mixed using the reversible mixer. It gives partial homogenization for more effective homogeneity during the mixing operation. This process has a cyclic reversal of the machine rotor and creates more effective agitating turbulence [8]. The paints mixing machines are many available on the world market but not all used to the small firm of automobile garages. The below table 1 shows the different types of paint mixing machines classifications.

Table 1. Machine classification with their disadvantages

S/N	Machine	Advantage	Disadvantage
1	Manual operated machine	Simple to operate even unskilled person	Less quality of mixed paint uniformity
2	High speed electrical operated paint mixer	Mixing high quantity in short time	Used to high demand manufacturing industries due and not affordable for small firm industries because of its cost
3	Computerised automatic mixing machine	High quality of mixed paints	High cost and need high skilled operators

This research article finds out the paint mixing method to overcome the disadvantages of the previously developed methods. This method is between manual and full- automatic mixing operations. The process of mixing is simple and human healthy. The developed paint mixing machine is simple to operate, easy for maintenance, and simple for transportation. The uniformity of paint color is easy to be obtained with vehicle body paint color standardized quality. The two methods have been used in this research. The first one is the design of the machine using Solid works software. The second method is an implementation of a physical model. This method starts with a preliminary measurement of machine structure components. The sizes of its parts fulfil the standards of mixer in line with dimensions of a reacting vessel, machine parts marking, metal cutting on sizes, sheet metal rolling and folding, and welding as the machine assembling mechanism during fabrication. The machine is electrically operated with high efficiency of auto-body color paints uniformity to the affordable cost.

2. Materials and methods

This fabricated paint mixing machine is semi-automatic machine because of its working principle. It is electrically operated and consists of various parts connected each other in a pre-designed manner and guided in a constrained way to obtain required outputs. This machine is designed in SolidWorks software and simulated in ANSYS software to the actual working environment for the finite element analysis of the machine structure to check its structure materials workability during machine operation. This machine structure frame is made by a strong steel cylindrical sheet metal designed to which is installed an A/C Single-phase Electric Motor with extended center shaft holder of two blades paint mixer designed to splash paint when rotating in the tank. The assembly is fixed on a strong stand made in tube of $20 \times 20 \times 1.6$ by welding. At the bottom of the cylinder, it has a van used to drain out the mixed paint. The detailed machine parts and their dimensions are shown in Table 1.

Table 2. Machine parts and dimensions

Part	Dimensions in mm		
Tank	Height *(H)*	Body dimeter *(D)*	Base dimeter (D_b)
	200	173	213
Motor	Shaft Length *(L)*	Shaft Dimeter *(d)*	Revolution *(N)*
	320	12	3000rpm
Mixer	Shaft dimeter *(d)*	Horizontal blade length *(B)*	Vertical blade length *(V)*
	12	148	101
Stand	Height *(h)*	Length *(l)*	Width *(w)*
	300	170	120

The design of a structural mechanism of the stand is based on the weight of the electrical motor, rotational speed, and vibration. And also, the mechanical properties of the mechanical structures have been taken under consideration. The considered properties are for the steel tubes and sheet metal. Due to steel is the main material used for machine structure. The designing consideration properties are strength, toughness, ductility, durability, weldability, and durability. The values taken was the maximum by minimizing machine maintenance cost [9]. The metal joining method used is a permanent joining by welding and temporally joining by bolting method. During assembling, the weldability factor has been considered based on joint cooling time, joint useful life, and workability resistance (corrosion, environmental effects, electrical motor resistance, and the total weight of the machine) from the International Organisation Standardization (ISO) report, ISO standard 2020 [10].

Figure 1. Assembled auto body paints mixing machine

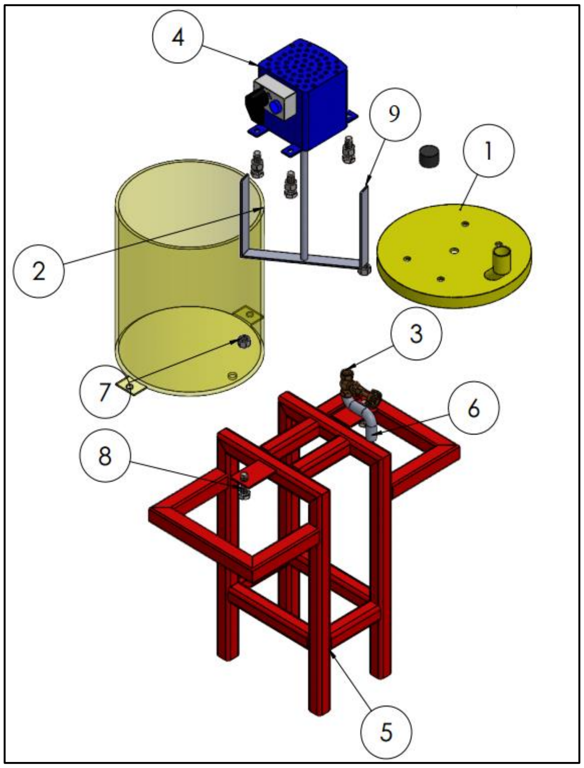

The motor has a blue color indicates that it was inserted from software features to the prescribed dimensions of the machine parts. Figure 1 illustrates the four tubes making a stand are well seated to facilitate good machine stability during operation. Hence all machine parts are available on the market at a low price. The importing mart is only an electrical motor. The way country's industrialization sector is starting to be developed, there is a hope that in a few years electrical motor will be available on the local market. But also, the motor doesn't increase too much the cost of the machine [11]. All joints of the stand are permanent by welding method. The assembling parts are illustrated in Figure 2. The assembling of electrical motor and tank is made by bolting, assembling of tank and stand is made by bolting while the pipes are fixed the tank using plumbing fittings.

The accessibility of machine parts or components is not complicated and makes the good maintainability of the machine. The assembling and disassembling are simple compare to the machines which have many hidden components. The mechanism of operation is designed to help in fault detection and repair which makes this machine to be friendly to operators. The machine dimensions like height from the ground are defined based on the average height of a human being for ease and comfort while operating the machine. The machine is painted to protect it against corrosion, sunlight, heavy rain, and keeping its exterior view [12]. The height of the machine is at the mean level to facilitate easy operability, also enough clearance is provided from the ground for cleaning purposes. This height doesn't affect the operating of the machine. The selection of materials was also based on machine weight. The machine weight is well defined to facilitate its transportation. The more garages in Rwanda work on vehicle body repair are not able to buy the machine but can rent it to make their finishing work to be attractive.

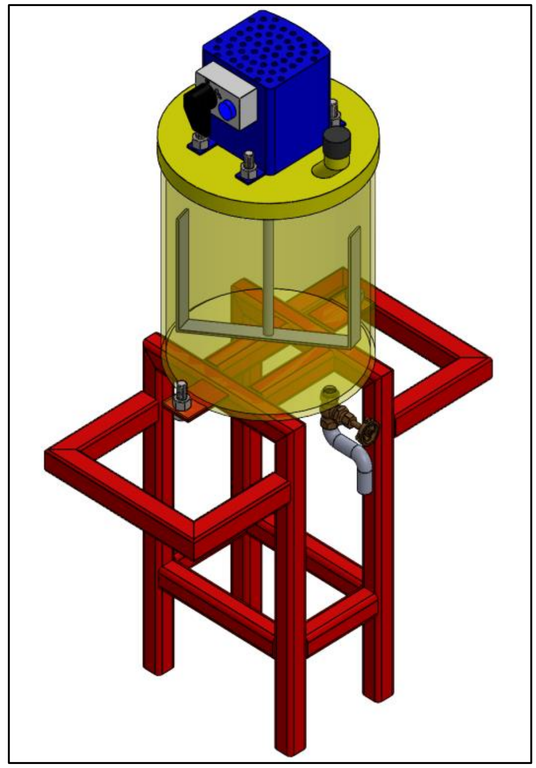

Figure 2. Machine parts drawn in solidworks (1. Cup for tank, 2. Tank, 3. Ball valve, 4. Assembled motor, 5. Stand, 6. Plastic pipe, 7. M8-S nut, 8. Bolt M8 and 9. Mixer blades)

The quantity of paint to be mixed depends the tank inter-nal volume and the revolution per minute of the electrical motor. The motor rotation is one of the parameters have been considered to facilitate the selection of a useful motor. The tank volume is calculated using the below equation to mitigate machine purpose.

$$V = \left(\frac{\pi D_b^2}{4} H\right)\left(\frac{\pi (D_b - D)^2}{4} H\right) \quad (1)$$

Where, $\boldsymbol{V}$ is the tank volume, $\boldsymbol{D}$ is the tank body diameter, $\boldsymbol{D_b}$ is the tank base dimeter, $\boldsymbol{H}$ is the height of the tank.

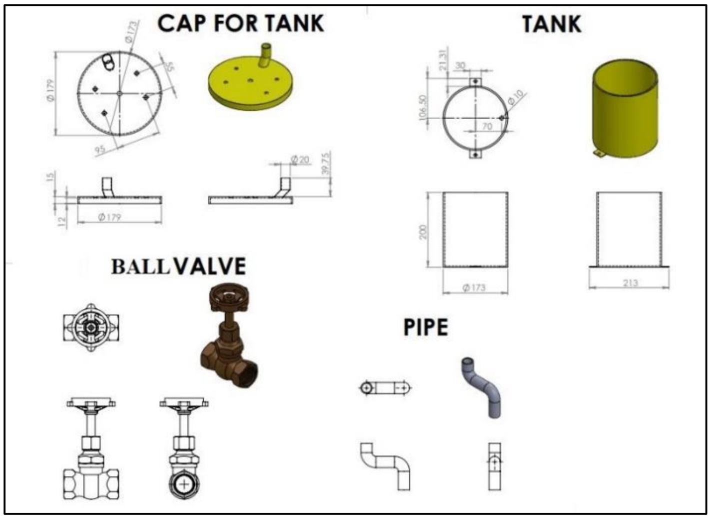

Figure 3: The most parts of the machine required attention checking and their view

3. Machine operation

The tank of the machine has a cylindrical shape and doesn't rotate. The rotating part is the shaft of the motor assembled with two tubes. During rotation of the motor shaft, these tubes rotate at the same speed as the shaft in paint and agitate all paint particles to form a similar species and form one color. The motor shaft is taken as the center shaft of the mixer and the assembled tubes are called mixer beaters. Hence the motor used is an alternating current motor type. The circular base of the hopper/ tank is assembled with a valve made by a short plastic pipe. This plastic pipe is used to take out the mixed paints from the tank after the mixing operation. The operation control including the electrical circuit breaker, control button (Switch ON/OFF) of the machine is fixed to the stand. When the machine is in the operation state there is a powerful lamp which is on and if the machine is in off mode the power is off.

The moving part has a predefined degree of freedom to make agitation of the paint mixture to the homogeneity output. The stability and vibration of the rotating part are well managed by the fixed parts (tank and stand). The machine uses an air-cooling system and it requires to be fixed in vent space to facilitate its cooling system. The steps of operating the machine are:

- Check the place to operate the machine is well flat and horizontal,
- Check if the stand is well seated on the ground,
- Check the connection of electricity to the electrical machine and the position of circuit breakers,
- Clean the tank using recommended solvent (Thinner or Petrol) and let it be dried,
- Open all the paint bags being mixed,
- Check all the valves if are well closed,
- Pour the paints in the tank and close the tank cover or cup properly,
- Switch on the machine and let work within 4 minutes switch it off and check the viscosity and color of the output mixture.
- If, it is well done, open full the valve and keep paint in a standardized prepared material
- Clean the tank before 2 minutes of removing the paints if you are not going to use the machine again with the same paint color or type.
- The operator of the machine should always have safety protective equipment.

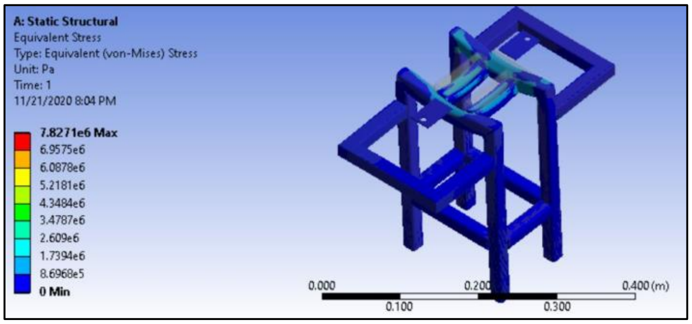

Figure 4. Machine stand Equivalent (von-Mises) stress (pa)

4. Results and Discussion

The stand of this machine is designed to support permanent load (the load of machine components) plus the variable load (load of paint in the tank to be mixed). The total load can't exceed 120kg. The stress concentration is on these two tubes fixing the tank and motor on the stand. However, the operability of the machine does not be affected by this stress. During operation, the stand can't reach the maximum stress. It works near to the minimum as it is shown in Figure 4. The maximum equivalent stress to be supported by the machine is 7.8271e6 Pa. At maximum load and motor speed, the maximum stress of the machine is 8.6968e5 Pa. It can't affect the operation of the machine stand. See Figure 4.

Figure 5 indicates the possible maximum and minimum deformation of the machine. The maximum deformation is 1.8022e-6 m at point application of the joint between the tank and the stand when the machine operates at maximum speed and load. This means that once the machine operates everyday none stop with maximum loads, two tubes fixing the tank should be replaced once a year. The option of adding the tube support to the verticals makes the machine operates well without reaching its maximum deformation. And instead of replacing the tubes joining the tank to the machine, the supports are replaced once in three years. It is the best option to keep the machine with a low maintenance cost. Figure 6 illustrates the variation of the stand metal deformation with the maximum frequency vibration of the machine. This implies that the deformation increases while the machine is not well seated to the horizontal plane. When vibration increases the deformation increase after 147Hz. Before 147Hz vibration can't affect the machine because the material properties have chosen to work with 180 RPM motor speed.

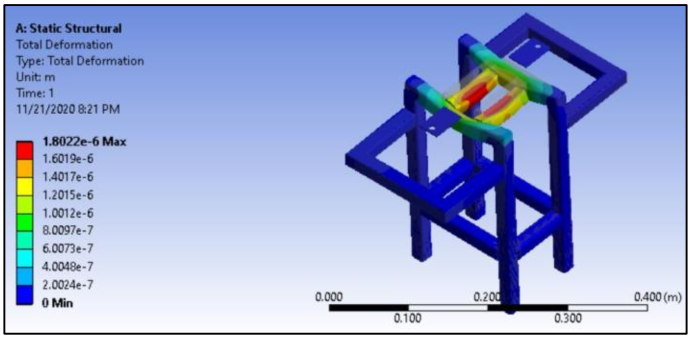

Figure 5. Total deformation of the machine stand

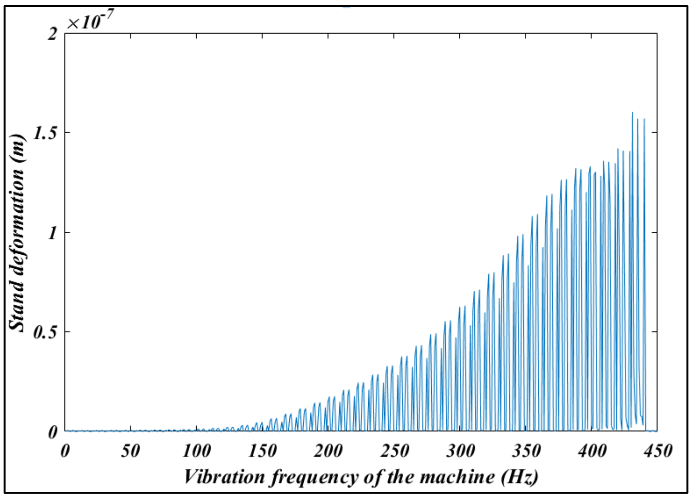

Figure 6. The stand deformation to vibration frequency of the machine

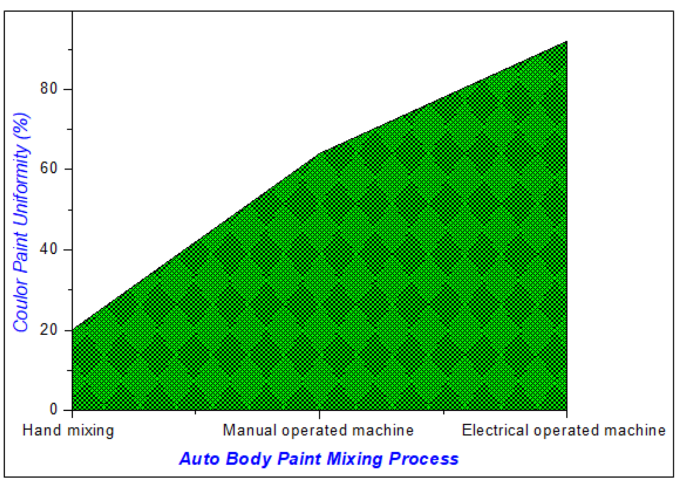

Figure 7. Auto body Painting uniformity

Figure 7 illustrates the operability of available mixing methods in Rwanda with the output's paints color uniformity. The comparative study of the auto-body paint mixing machines available in the Rwanda market shows that this electrically operated machine performs well compare to other mechanical operated machines and hand mixing method. This machine doesn't have 100% paint uniformity. It reaches 91% paint mixture uniformity.

The analysis was base to the practices we did in the manufacturing workshop during the all-manufacturing process of this machine. There used the hand mixing method and manually operated mixing machine. We took 8 samples of paint mixture from 4 paint colors to have one uniform paint color used to paint on a monocoque vehicle body. The obtained results show that the quality of color uniformity of the two methods (hand mixing and manual operated) is too low and took more time of mixing process compared to this machine. None goes up to 65% of color uniformity. This electrically operated machine uses only 1/14 of the total time other methods to get the required attractive color paint uniformity.

5. Conclusion

In this research, the study of paint properties has done to meet the designing and fabricate paint mixing machine that is able to mix paints with different colors to the single attractive color of the vehicle body. The machine works above 90% of color uniformity at high speed and its cost is affordable. The auto body repair will be improved and to use this machine is to save more time and attracting the customers to use the garage. As the need for paint production has a high increasing rate in the country, this then becomes our reason for the fabrication of an electric motor is driven paint mixer. It solves the problems of Rwanda's automotive garages. However, it is a good solution to producing local paint mixing machines that can serve our society. The future works are to improve its mixture uniformity to 100% and increasing the maximum load capacity to be mixed for one round.

Conflict of Interest Statement

The authors declare that there is no conflict of interest.

CRediT Author Statement

Frederic Musabyimana: Supervision, methodology, article editing, Writing original draft and revision; **Pacifique Turabimana:** Methodology, article editing, Writing original draft and revision.

Acknowledgements

We would like to acknowledge the Rwanda Polytechnic for the funds provided in carrying out this project through its initiative of supporting research projects by equipping the workshops where we did our prototype models and physical model. We want also to acknowledge the IPRC Kigali workshop instructors for their exceptional collaboration during the implementation of this auto body paint mixing machine.

References

1. Gerlock, J. L., Kucherov, A. V., & Smith, C. A. (2001). Determination of active HALS in automotive paint systems II: HALS distribution in weathered clearcoat/basecoat paint systems. Polymer degradation and stability, 73(2), 201-210.
2. Jones, F. N., Nichols, M. E., & Pappas, S. P. (2017). Organic coatings: science and technology. John Wiley & Sons.

3. Han, Y. H., Zhou, C., Bras, B., McGinnis, L., Carmichael, C., & Newcomb, P. J. (2003). Paint line color change reduction in automobile assembly through simulation. In Winter Simulation Conference (Vol. 2, pp. 1204-1209).
4. Akafuah, N. K., Poozesh, S., Salaimeh, A., Patrick, G., Lawler, K., & Saito, K. (2016). Evolution of the automotive body coating process—A review. Coatings, 6(2), 24.
5. Richard C.G., (2018) "Development of a Paint Mixing Machine," International Journal of Academic Engineering Research, 2(4), 9-16.
6. Pfanstiehl, J. (1998). Automotive paint handbook: paint technology for auto enthusiasts & body shop professionals. Penguin.
7. Lacey J. (2009). Occupational Exposures in Paint Manufacturing and Painting," Petroleum distillate Solvents.
8. Scicolone, J., Mujumdar, A., Sundaresan, S., & Davé, R. N. (2011). Environmentally benign dry mechanical mixing of nano-particles using magnetically assisted impaction mixing process. Powder technology, 209(1-3), 138-146.
9. Davison, B., & Owens, G. W. (Eds.). (2012). Steel designers' manual. John Wiley & Sons.
10. STANDARD, B. (2002). Welding—Recommendations for welding of metallic materials—. Change, 13981, 30.
11. Omorusi, I. I. (2020). Design and Construction of an Electrically Operated Paint Mixing Machine. Journal of Engineering Research and Reports, 20-29.
12. Castano, C. E., Fahrenholtz, W. G., & O'Keefe, M. J. (2020). Ceria-based coatings and pigments. Cerium Oxide (CeO_2): Synthesis, Properties and Applications, 211-257.

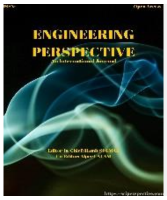

e-ISSN:2757-9077

ENGINEERING PERSPECTIVE

https://sciperspective.com/

Research Paper

Optimization of concrete sleepers subjected to static and impact loadings

Ndabamenye Theogene [1], Ntakiyemungu Mathieu[1*] and Abrham Gebre[1]

[1]*African Railway Center of Excellence, Addis Ababa Institute of Technology, Addis Ababa University, Ethiopia*

ABSTRACT

Prestressed concrete sleepers play an essential role in the railway track's performance and safety responses, having an important function of transferring and distributing loads from the track's superstructure to ballast bed. Cracks on the prestressed concrete sleepers are mainly caused by impact loadings form wheel and rail interactions. Thus, the excessive railway track maintenance cost. The effect and optimization of different prestressed sleeper shape under static and impact loadings has not been previously well investigated. Therefore, this paper focused on the optimization of prestressed concrete sleepers (PCS) shape looking at sleeper safety and sleeper volume. ANSYS 16 was used to analyze the static and impact loading on sleepers. The concrete part of the sleeper was modelled using a three-dimensional solid element, SOLID65 and the pre-stressing wires by truss elements, LINK180, to withstand the initial strain attributed to pre-stressing forces. This paper revealed that irregular hexagon sleeper shape with different width at rail seat and center section having 251 mm and 175 mm center width and height respectively; 281 mm and 200 mm end and rail seat width and height respectively is safe. This paper; thus, point out to irregular hexagonal shape sleeper are more economical and safe unlike the other modelled shapes.

Keywords: Prestressed concrete sleeper; static and impact loadings; ANSYS, Finite element; optimization

History
Received: 04.07.2021
Accepted: 21.08.2021

http://dx.doi.org/10.29228/eng.pers.52117

Author Contacts
**Corresponding Author*
e-mail addresses : ntakmatnty@gmail.com, ninitha2020@yahoo.com, abrhamgebre16@gmail.com
Orcid numbers : 0000-0003-4862-8940, 0000-0001-9872-9040, 0000-0003-0172-2905

1. Introduction

Sleepers form an integral part of the railway superstructure track components that help in transmission of rail vertical loads to the substructure. As reported by [1], the most important functions of railway sleeper include the transfer and distribution of vertical loads from superstructure to foundation, restrain of lateral, longitudinal and vertical movement of rails. Cracks in concrete sleepers are due to impact loading caused by wheel/rail interaction with or without wheel/rail irregularities. [2, 3 &4], noted that impact loads appear in short duration but of very high magnitude wheel loads due to abnormalities on the wheels and or on the railhead surface. Prestressed concrete sleeper (PCS) was analyzed numerically and analytically by different researchers. The analytical and numerical method was conducted by [5], to analyse and optimize a PCS by varying one shape dimensions of the existing sleeper. Concrete grade, and tendon (wire) type and profile were considered. Moreover, [5] did not consider impact loading in the design and other sleeper shapes like rectangular, hexagonal sleeper sections. Prestressed concrete sleeper was optimized by [6] considering different dimensions and pressure distribution beneath the sleeper. In the analysis, only one cross section shape has been used, others cross section shape at both rail seat and center of sleeper were overlooked. Optimization of prestressed concrete sleeper has been conducted by [7] using sensitivity analysis with different sleepers so as to determine the number and position of rebars. Studies on different sleeper shapes and dimensions were overlooked. The effect and optimization of different prestressed concrete sleeper shape subjected to both static and impact loading were not previously well investigated. PC design has utilized the permissible stress principle taking into account only the static and quasi-static loads used in the design of PC sleepers, thus not tolerating the small sleeper cracks due to large spikes from track loading. Cracked sleepers must be replaced by new sleeper, that make the railway maintenance very costly. The main objective of this study is to numerically investigate the behaviour of concrete sleeper and optimize sleeper shape subjected to static and impact loadings.

2. Optimization formulation

Optimization is defined as the selection of the best element which can be cost, profit, quality, safety or environment impact; from some set of available alternatives. In this paper, optimization was conducted to ensure the sleeper safety and volume. In this case, two objective functions are analyzed. As reported by [8]; to transform a multiobjective optimization problem into a single objective; weighted sum method could be used. Objective functions such as sleeper safety and sleeper cost in times of sleeper total volume are given as $f_1(x)$ and $f_2(x)$ respectively. Combining the two, the following scalar objective is given as:

$$F(x) = \alpha_1 f_1(x) + \alpha_2 f_2(x) \quad (1)$$

Where, α_1 and α_2 are the weighting coefficients with $\alpha_1 + \alpha_2 = 1$, α_1 and α_2 are from literatures. According to [9], in his study; a rail safety of 59% was reported with 41 % cost. The sleeper safety is based on the way the sleepers behave under both static and impact loading. Bending stress at top and bottom has to be considered and compared to the permissible stress provided by AS 1085.14 [10]. The sleeper volume was also taken into account. The weighted sum method was used to select the best geometrical sleeper shape. The two objective functions (safety and volume) are formulated from ANSYS software after importing some parameter into the software.

3. Model Validation

Static sleeper model was modelled, analyzed and compared with Rikard (2000) model [11]. ANSYS 16 was used to simulate the behaviours of a sleeper. Three-dimensional solid element, SOLID 65 was used to model concrete part which has the material model to predict the failure of brittle materials. To simulate the behaviour of prestressing wires, truss elements, LINK180, were used to withstand the initial strain attributed to prestressing forces, by assuming perfect bond between these elements and concrete. Sleeper was subjected to the same hydraulic jack loading as Rikard model (2000). The load is applied to the rail seat area varying from 0 to 237.5 kN. The vertical deformation as shown in figure 1 at a load of 237.5 kN shows symmetry of the sleeper at the centre and it shows the maximum directional deformation. It is clear from the load-deformation graph (figure 2) that the force and deformation diagram matches very well to the Rikard (2000) model which proves that the quality of the FE results is good. Therefore, further modelling and analysis using FEM follows in the next sections of the paper.

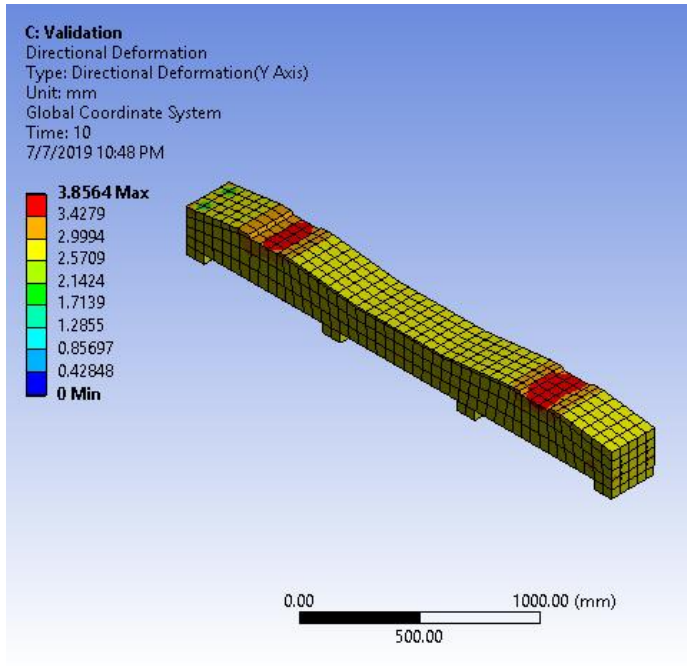

Figure 1. Deformation at 237.5 kN

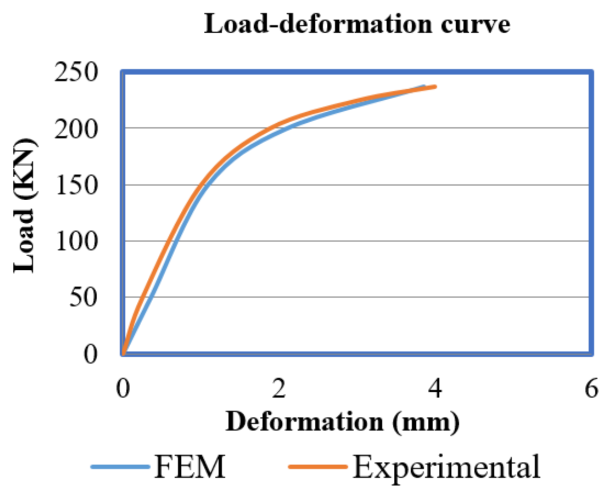

Figure 2. Force - Deformation graph

4. Numerical Model

4.1. Geometrical shape and dimensions of modelled sleeper

Different cross sections of sleeper at both rail seat and center were selected: trapezoidal, rectangular, and irregular hexagon cross section, taking into account the variation in sleeper size. The sleeper is symetric in shape and size about its centre portion. The selections of sleeper dimensions were first based on the minimum values of bottom and top width at both rail seat and center section and minimum height. Using the equation proposed by Australian Standard (2003) [10], the rail seat load was computed as 159.375 KN based on the axle load of 25 tones, distribution factor of 0.51 and impact factor value of 250% proposed by

[4,10]. Minimum bottom width, top width and height were limited to 255 mm, 168 mm and 160 mm respectively. Existing sleeper used by Ethiopian Railway Corporation (ERC) [12] was considered and its corresponding volume, surface was computed as 0.1139 m3 and 0.68 m2 respectively. Sleeper having same volume, soffit area, heights, volume and soffit area, volume and heights, soffit area and heights as the existing sleeper were considered as constraints. The excel random between functions between the minimum and the maximum dimensions, was used to generate the random geometrical parameters. In addition to this, the moment of inertia at both sleeper rail seat section and center section was taken also as the basis of the sleeper selections. Therefore, fifteen models with their corresponding dimensions were selected.

4.2. Material properties

The concrete grade C60 and prestressing steel wire of 7 mm diameter was used in this paper. The maximum permissible stress in concrete after allowing all losses of prestress were proposed by [4,10] and in compression and in tension, the formula of $0.45 * f_c^{'}$ and $0.4 * (f_c^{'})^{0.5}$ was proposed respectively. The value of stress for stretching prestressed reinforcement in the steel wire of $0.75 * f_{plk}$ must be used as proposed by Chinese Standards [13]. Therefore, a use of characteristic strength and young modulus of steel wire of 1,570 Mpa and 200,000 Mpa was proposed. The initial strain of 0.00058875 m/m = 5.8875 mm/m was also computed. Table 1 shows in details the for concrete and prestressing wires properties.

Table 1 Material properties of concrete and prestressing steel [11,13,14]

S/N	Properties	Concrete	Prestressing wires
1	Density (φ_c), kg/m3	2400	7,800
2	Young's modulus, (E_c), Mpa	37,720	200,000
3	Poisson's ratio (μ_c)	0.2	0.3
4	Thermal expansion (α_c), /c	$1*10^{-5}$	-
5	Strain value	0.003	0.00542
6	Yield strength (Mpa)	55	1,750
7	Tensile strength (Mpa)	2.85	1,085
8	Shear transfer	0.9	-
9	Characteristic strength (Mpa)	60	1,570

4.3. Prestressed concrete sleeper modelling

4.3.1. Static analysis in ANSYS

Sleeper modelling was conducted with ANSYS 16.0. For analysis purposes, since the sleeper was symmetric, a half sleeper was considered. Hex dominant meshing method was used for all models with mesh size of 25 mm for all models (figure 3). The support of the sleeper is modelled as a spring, as per (Shan, 2012) and [15]. For all cases, the ballast stiffness was computed considering two layers; ballast and sub-ballast. As per [16]; the distribution angles for both ballast and sub-ballast are assumed to be 30 degrees and 35 degrees respectively for the two layers with 300 mm and 200 mm thickness respectively. The corresponding elastic moduli for the two thicknesses are 200 Mpa and 150 Mpa respectively,[17,18]. A set of solutions are available in ANSYS such as deformation (total or directional) and stresses (equivalent, and shear). The relationship between the three stresses was reported by [19] when the normal stress in times of bending stress was converted into an equivalent stress.

With σ_V = Equivalent (Von-Mises) stress, σ_b = bending stress and σ_s = shear stress, then

$$\sigma_b = \sqrt{(\sigma_V)^2 - 3*(\sigma_s)^2} \quad (2)$$

4.3.2. Explicit dynamics in ANSYS

Explicit dynamic in ANSYS Workbench was used to model impact loadings so as to analyze impact analysis of prestressed concrete sleeper (figure 4). The model is hammered by the impactor that generates an impact force when it is given an initial velocity. The velocity given to the impactor and its contact to the element to analyze, creates an impact force.

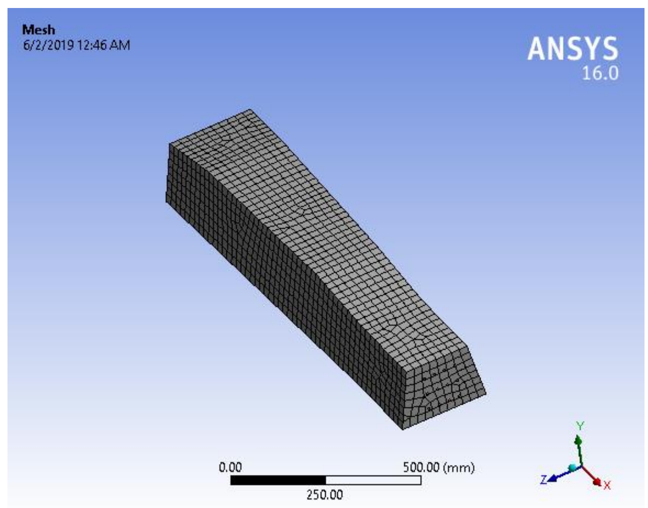

Figure 3. Hex dominant mesh method

The mass of the impactor is taken as the mass of the wheel as reported by [4&15]. It was assumed that the rail and the impactor are made of steel that bear similar properties according to [4]. The same meshing method and element size used in static structural analysis was maintained for explicit dynamics analysis. In this paper, the same properties used for static structural analysis are assumed to be same for explicit dynamic analysis corresponding to both concrete and prestressing wires. The drop velocity was 1.373 m/s equivalent to 0.1m drop height. The initial velocity on the impactor was set so that the impact event on the sleeper is created. The ballast stiffness used to support the sleeper is not supported by explicit dynamics, hence, the fixed support was assumed for all models which don't affect the stress result.

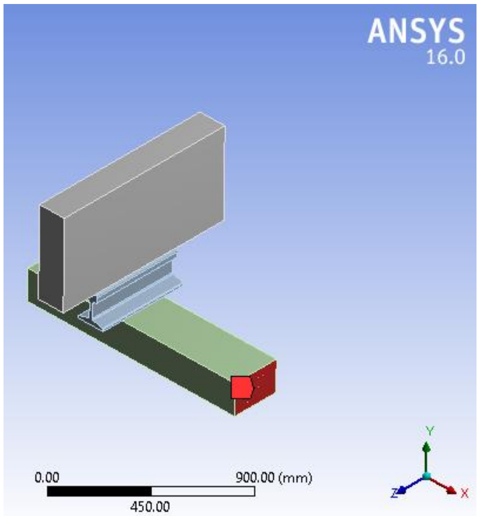

Figure 4. Model geometry

5. Results and Discussions

In this section, the analysis results of all models are presented to obtain the deformation and stresses for different sleepers. Stresses and deformations at rail seat were considered, results at center and end section were not considered in the analysis as they were too small.

5.1. Static results

In ANSYS 16, static structural analysis determines the displacements, stresses, strains, and forces in structures or components caused by loads. Critical sections such as the rail seat, center and end sections were emphasized and maximum deformation and stresses in concrete are located at rail seat section. The higher total deformation and stresses are located at rail seat section and at end and center sections are too small compared to the rail seat results. The equivalent stresses and shear stresses were recorded from ANSYS 16.0 and the corresponding bending stresses were computed based on equation 2. Both total deformation and stresses are shown in figure 5, 6 and 7. The lower deformation is located in rectangular section sleeper (SL-2) and (SL-5), whereas the higher pick values at sleeper, (SL-7). As shown in Figure 6 and 7; the higher bending stress at top sleeper section were located in sleeper (SL-4) followed by sleeper (SL-10) while the lower value to sleeper to sleeper (SL-1) followed by sleeper (SL-8) and ((SL-13). The higher bending stress at bottom rail seat section was located to sleeper (SL-5) followed by sleeper (SL-10) and the lower value at sleeper (SL-70. The results in Figure 6 and 7 shows that all modelled sleeper resist the static loadings imposed on them. Therefore, all selected sleepers are safe.

5.2. Impact results

The impact simulations were conducted on fifteen models. The total deformation and bending stress are also shown in figure 5, 6 and 7. The lower pick deformation is located in rectangular section sleeper (SL-2) and (SL-5), whereas the higher pick at trapezoid sleeper section, (SL-6) and irregular hexagon sleeper section, (SL-8). The equation 2 has been used to compute the bending stress. The higher bending stresses at top sleeper section were located in sleeper (SL-8) while the lower value to sleeper (SL-2) and (SL-5). The higher bending stress at bottom rail seat section was located to sleeper (SL-5), (SL-2) while the lower values to sleeper (SL-9) and (SL-13). The sleeper: (SL-7), (SL-8), (SL-9), (SL-11) and (SL-13) was found to be safe. The similarities from SL-1 to SL-6 found in figure 5 for deformation of those sleepers subjected to both static and impact loadings is due to the similar shape of the sleeper base.

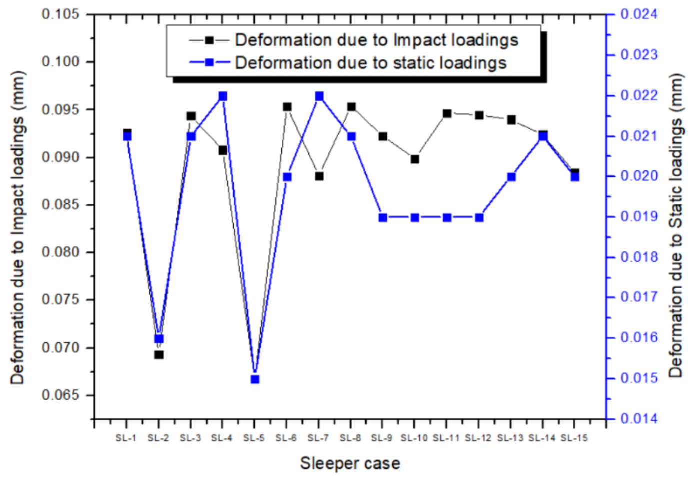

Figure 0. Deformation due to both static and impact loadings

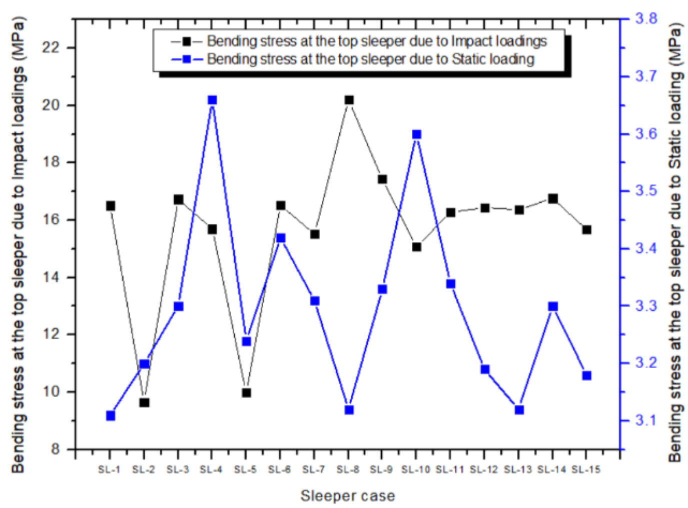

Figure 6. Bending stress at top sleeper due to both static and impact loadings

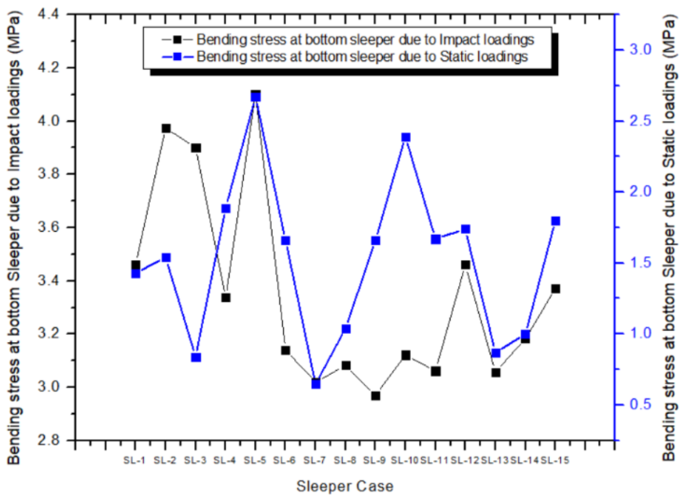

Figure 7. Bending stress at bottom sleeper due to both static and impact loadings

5.3. Selection of the best geometrical sleeper shape

5.3.1. Ranking the sleeper according to safety

Safety ranking was based on bending stress in comparison with the permissible stresses. The total deformation was not considered in the analysis as they are qualifying very small values as shown in figure 5. The bending stress has to be lower than the permissible stresses provided by Australian standard [10]. Therefore, the ratio between the permissible stresses and the bending stresses should be greater than 1. The corresponding permissible stress in compression and tension are 27 Mpa and 3.1 Mpa respectively. Ratios for the selected five sleepers were computed for the sleepers as shown in table 3 with their corresponding safety ranking. To evaluate and rank the consideration of the criteria in theses sleepers;a value of 1 to 5 was assigned to the selected sleeper. The two objective functions (compression and tension) contributing to the overall ranking, are having equal coefficient. Therefore, the overall ranking was computed with the summation of the two objective functions values. Rank one was given to the lower value as shown in table 2. The sleeper with lowest overall ranking was selected as the safest sleeper to resist impact loadings.

The static results were reviewed against safety for the sleeper shown in table 2 above. Respective individual ratios and ranking are shown in table 3. The overall safety ranking as far as static loadings are concerned, were computed in the similar procedures as for impact results. The overall safety ranking combining both static and impact results is shown in table 4. Investigations made on the sleeper able to resist the applied impact loadings showed that sleeper (SL-7) of irregular hexagon shape with a varying width was the safest compare to the other selected sleeper shapes. Sleeper (SL-13) was the safest when the static loadings were considered. The selected sleeper was of rectangular sections, trapezoid sections and irregular hexagon sections. Among those models; the irregular hexagon sections were the safest sleeper shape as far as the impact loading and static loading are concerned.

Table 2 Ratio of permissible and bending stress according to impact results and safety ranking

Sleeper Cases	Top Bending Stresses (Mpa)	Ratio	Ranking	Bottom Bending Stresses (Mpa)	Ratio	Ranking	Sum of rankings	Overall ranking
SL-7	15.52	**1.74**	**1**	3.02	**1.026**	**2**	3	**1**
SL-8	20.20	**1.34**	**5**	3.08	**1.006**	**5**	10	**4**
SL-9	17.43	**1.55**	**4**	2.97	**1.044**	**1**	5	**2**
SL-11	16.28	**1.66**	**2**	3.06	**1.013**	**4**	6	**3**
SL-13	16.38	**1.65**	**3**	3.056	**1.014**	**3**	6	**3**

Table 3 Ratio of permissible and bending stress according to static results and safety ranking

Sleeper Cases	Top Bending Stresses (Mpa)	Ratio	Ranking	Bottom Bending Stresses (Mpa)	Ratio	Ranking	Sum of rankings	Overall ranking
SL-7	3.306	**8.166**	**3**	0.647	**4.795**	**1**	4	**2**
SL-8	3.122	**8.648**	**2**	1.040	**2.982**	**3**	5	**3**
SL-9	3.333	**8.100**	**4**	1.660	**1.868**	**4**	8	**4**
SL-11	3.336	**8.095**	**5**	1.672	**1.854**	**5**	10	**5**
SL-13	3.117	**8.663**	**1**	0.872	**3.553**	**2**	3	**1**

Table 4 Safety ranking according to both static and impact results

S/N	Sleeper Cases	Safety ranking as per static results	Safety ranking as per impact results	Sum of rank-ings	Overall ranking
1	**SL-7**	2	1	3	**1**
2	**SL-8**	3	4	7	**4**
3	**SL-9**	4	2	6	**3**
4	**SL-11**	5	3	8	**5**
5	**SL-13**	1	3	4	**2**

5.3.2. The total volume of the selected sleeper

Total number of sleepers modelled for static and impact simulations are fifteen. As far as impact results are concerned, five sleepers were selected to be safe. The corresponding total volumes and ranking were shown in table 5. It shows that the lower the volume, the lower the ranking number

Table 5 Total volume of the selected sleepers and their ranking

S/N	Sleeper Cases	Volume (m^3)	Ranking
1	SL-7	0.11419	**4**
2	SL-8	0.11421	**5**
3	SL-9	0.11215	**2**
4	SL-11	0.11366	**3**
5	SL-13	0.11211	**1**

The overall sleeper safety and volume ranking was computed according to equation 1. The objective functions are shown in table 4 and 5, the weighting coefficients are given as 0.59 (59%) and 0.41 (41%) for sleeper safety and sleeper volume respectively. As shown in table 6, the sleeper having the lower sum of ratings was considered as the best geometrical sleeper shape. Therefore, Sleeper (SL-13) having a sum of ranking of 1.59 was recommended as the best geometrical sleeper shape (figure 8), which was characterized by a different width at both the center and rail seat sections. In comparison to the existing sleeper (in the Addis-Djibouti railway track) in Ethiopia; the best geometrical sleeper shape has a 1.75% volume reduction. Irregular hexagon forms a sleeper that is safe compared to sleepers of other shapes considered in this research.

Table 6 Best geometrical sleeper shape selection

S/N	Sleeper Case	Sum of rankings	Overall ranking
1	**SL-7**	**2.23**	**2**
2	SL-8	4.41	5
3	SL-9	2.59	3
4	SL-11	4.19	4
5	**SL-13**	**1.59**	**1**

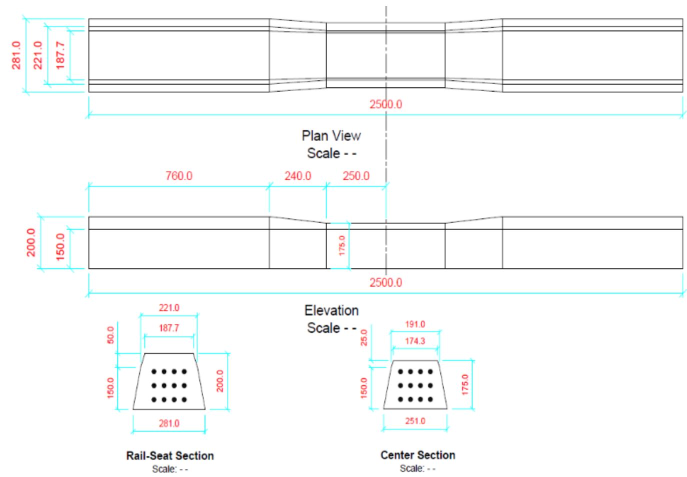

Figure8. Best geometrical sleeper shape

6. Conclusion

Results from static simulation revealed that rectangular sleeper shapes are having the lower top stress and higher bottom stress compare to the other sleeper shapes. The trapezoid and irregular hexagon sleeper sections are having lower stress compare to rectangular sections. However, impact simulation's results proved that the irregular hexagon sleeper shapes resisted impact loadings much better compared to the other sleeper shapes. Optimization of sleeper was based on the criteria of sleeper safety, and sleeper total volume. Analysis results showed that the best geometrical sleeper shape was (SL-13) of an irregular hexagon with different widths at rail seat and center sections; 251 mm center width, 281 mm end and rail seat width, 175 mm height at center section and 200 mm height at end and rail seat sections. As per this research, the sum of rankings that included sleeper safety, cost in times of total volume for the best geometrical sleeper shape was 1.59. Sleeper (SL-7) was the next best geometrical sleeper shape with a similar ranking sum of 2.23. The shape of sleeper (SL-7) was an irregular hexagon with a varying width from center to end sections, having 248 mm as center width, 308 mm on the end section, 171 mm height at center section and 207.8 mm height at end and rail seat sections. This paper points out to irregular hexagonal shape sleepers to be economical and safe. Therefore, sleeper model (SL-13) that has an irregular hexagon shape is proposed for use on future extension of the existing lines and or in the construction of new lines. Future research in regards to concrete sleeper optimization are proposed to ensure the proper lateral stability; incorporating other track components such as rail, rail pad, ballast and subgrade as part of railway track system in order to better comprehend the effect of these components to the sleeper. To ensure both safety and fair sleeper manufacturing and material, sleeper cross-sectional and front view dimensions are recommended for further optimizations. Laboratory investigations are also recommended to be conducted in future.

Conflict of Interest Statement

The authors declare that there is no conflict of interest.

CRediT Author Statement

Ndabamenye Theogene: Writing original draft and revision, **Ntakiyemungu Mathieu**: article editing and revision, **Gebre Abrham**: Supervision, article editing and revision.

References

1. Li, D., Kaewunruen, S., & Robery, P. (2017). Creep and shrinkage effects on Railway Prestressed concrete sleepers. First international conference on rail transportation-ICRT 2017, (pp. 1-8). Chengdu, China.
2. Kaewunruen S. & Remennikov A. (2007). Experimental and Numerical Studies of Railway Prestressed Concrete Sleepers Under Static and Impact Loads. Civil Computing, 3, 25-28.
3. Kaewunruen, S., & Remennikov, A. (2013). On the residual energy toughness of prestressed concrete sleepers In railway track structures subjected to repeated impact loads. Electron. J. Struct. Eng., 41-61. engineering, Chalmers University of Technology.
4. S. Kaewunruen. (2007). Experimental and numerical studies for evaluating dynamic behaviour of prestressed concrete sleepers subject to severe impact loading,. PhD thesis, UoW, Aust.,.
5. Desalew, F. (2014). Analysis and Design of Prestressed Concrete Sleeper. Addis Ababa , Ethiopia.: Master's Thesis in Civil Engineering in the Graduate Studies, Addis Ababa Institute of Technology, Addis Ababa University, Addis Ababa , Ethiopia.
6. Sadeghi, J., & Babaee, A. (2006). Structural Optimization of B70 railway prestressed concrete sleepers. Iranian Journal of Science & Technology, Vol.30.,No.B4 School of Railway Engineering, Iran University of Science and Technology, Tehran, LR of Iran.
7. Minoura, S., Wantanabe, T., Sogabe, M., & Gato, K. (2017). Analytical Study on Loading Capacity of Prestressed Concrete Sleeper. Procedia Engineering.
8. Yang, X.-S. (2010). Engineering optimization, an introduction with Metaheuristic applications, . United Kingdom: University of Cambridge, Department of engineering, Cambridge, A JOHN WILEY & SONS, INC.,PUBLICATION
9. Johan, B. (2002). Railway Safety-Risk and economics,. PhD's thesis, Department of infrastructure and planning, Royal Institute of Technology, ISSN 1651-0216.
10. AS. (2003). Australian Standard, AS 1085.14 "Railway track materials", Part 14: "Prestressed Concrete Sleepers".
11. Rikard G. (2000). Static and dynamic finite element analysis of concrete sleepers. Göteborg, Sweden: Department of structural
12. Corporation, E. R. (2012.). Ethiopia/Sebeta-Djibouti/Nagad Railway Feasibility Study-Part 1: General Specifications Executive Edition,.
13. Chinese, S. (2002). National Standard of People's Republic of China: Code of Design of Concrete Structures. GB50010-2002.
14. Shan, L. (2012). Railway Sleeper Modelling with Deterministic and Non-deterministic Support Conditions. Master Degree Project.
15. Hong Lim, C., Kaewunruen, S., & Mlilo, N. (2017). Performance of Railway Sleepers with Holes under Impact Loading. IOP Conference Series: Materials Science and Engineering 280., pp 1-6.
16. Ahlebeck, D., Meacham, H., & Prause, R. (1975). The development of Analytical models fro railroad track. Proc., Symposium on Railroad Track Mechanics (A. D. Kerr, ed.),, (pp. pp. 239-261).
17. Jabbar Ali, Z., & Seyed Ali, M. (2016). Study of ballast layer stiffness in railway tracks. pp. 311-318.
18. Bowles, J. (1988). Foundation Analysis and Design. . New York.: Fourth edition, McGraw-Hill Book Company, .
19. Ivanov, I., & Corves, B. (2014). Fatigue testing of flexure hinges for the purpose of the development of high-precision micro manipulator. "Mechanical Sciences; department of mechanism theory and dynamics of machines (IGM), RWTH Aachen University, Aachen, Germany, pp.59-66.